BACHELOR'S THESIS

Variability in modelled Arctic Sea-Ice Volume

Author:
Hanna AXÉN[1]

Supervisors:
Dirk NOTZ[2]
Erik SWIETLICKI[1]

Autumn Semester 2013

[1]Lund University
[2]Max Planck Institute of Meteorology

Abstract

In this thesis, the Arctic sea ice volume and thickness evolution over the time period 1850-2100 is analysed. The analysed data is provided by the CMIP5 climate models, which contributed their output for the IPCC Fifth Assessment. The results were compared to the re-analysis data series PIOMAS. Three RCP projections, with different greenhouse gas emission scenarios, were used for the time period 2006-2100. The change in seasonal cycle was investigated throughout the time period and for the three RCP scenarios. Two of the models were evaluated in more detail, these were MPI-ESM and EC-EARTH. Maps showing the thickness change, according to the two models MPI-ESM and EC-EARTH, were made.

The evolution of the sea ice volume shows a dependence on the change in radiative forcing, thus the emissions of greenhouse gases. For the high emission scenario, ice-free conditions in September are reached before 2100. The models are able to reproduce some characteristics of the sea-ice, but are generally underestimating the total volume. The most important finding is that none of the models is able to reproduce the rapid decrease in volume which is seen in PIOMAS and supported by observations. This indicates that there is some component missing in the models. The sea-ice retreat can also be expected to go faster than seen in the models if greenhouse emissions are not decreased.

The reduction would, according to the models, slow down when the ice gets thinner, since thick ice reacts stronger than thin to changes in radiative forcing. The models show that the sea-ice would have some quasi-equilibrium, depending on the climate, and no so called tipping point after which the sea-ice would not be able to recover. It would then still be possible for us to stop further sea-ice reduction.

Acknowledgements

First of all I want to thank my supervisor Dirk Notz, at Max Planck Institute of Meteorology, who made it possible for me come to Hamburg and conduct this thesis. His admirable passion for what he is doing and patience in teaching has helped me a lot. I also want to thank my supervisor at Lund University, Erik Swietlicki, for his support and helpful comments during my work.

A special thanks to Patrick Fink for taking care of me and letting me stay in his apartment during my Hamburg visit. Also thanks to all the helpful people at MPI for explanations and inspiration, and to the Department of Physics and Division of Nuclear Physics at Lund University for financial support.

Thank you Wilhelm May for helping me with the shell scripts when I got back to Lund.

Thanks a lot to my family and friends for all the support you have given me. Especially my dad, Göran Axén, and my uncle, Lars-Erik Röjerås, who read and gave comments on my thesis.

Thank you!

Contents

1 Introduction

In this thesis I analyse the Coupled Modelling Comparison Project 5 (CMIP5) climate models' sea-ice output. I have evaluated how the models predict the sea-ice volume and thickness, and compared this to observations.

Two of the models were evaluated in more detail: Max Planck Institute for Meteorology's Earth System Model (MPI-ESM) and EC-EARTH, an earth system model from the European Centre for Medium-range Weather Forecast (ECMWF). EC-EARTH is a global coupled climate model which has contributions from Lund University, my home university. MPI-ESM is made by people at Max Planck Institute, including my supervisor Dirk Notz. Therefore these two models were of extra interest for me. I have compared how the seasonal cycle for these two models is changing through the time series compared to the multi-model mean. Finally I have investigated where the thinning is most pronounced according to the two models, MPI-ESM and EC-EARTH.

1.1 Background and Motivation

The Intergovernmental Panel's on Climate Change (IPCC) fifth Assessment Report, released this September (2013), clarified how anthropogenic greenhouse gas emissions affect the earth's climate system, with changes in e.g. temperature, sea-level, precipitation and circulation patterns, snow and ice cover, as effect. Discussion concerning climate change may now be more important than ever. The sea-ice is a critical part of the climate system as the link between ocean and the atmosphere around the poles, but changing ice conditions do also have a direct effect on the people living in its vicinity. The sea-ice is used for travelling and hunting, which implies major lifestyle changes as the ice retreats, not to forget the affects on entire polar ecosystems, in which species are highly adapted to these unique conditions. There are polar bears, walrus, seals, narwhal, microbial communities and different migration species, all dependent on the sea-ice for their living. The effect of sea-ice reduction could thus be on the biodiversity both regionally and globally (AMAP, 2012).

Less sea-ice cover enables shorter shipping routes through the Arctic, which could reduce the emissions. Though, there is a possibility of increased industrial activities in the Arctic region, which could be harmful to the sensitive and already threatened ecosystems.

More open ocean enables more wind stress and wave activity. This increases erosion, as has been reported from e.g. Siberia and Alaska (Serreze et al., 2007). The sea-ice importance as a climate indicator and its effects on

the climate system globally, will be discussed further in the next section.

It is of great importance to understand the behaviour and responses of sea-ice, which is why I choose this topic for my thesis.

1.2 Theory

1.2.1 Sea-ice Thickness Changes

Although the global-mean warming trend has diminished over the last decade, temperatures continue to increase in the Arctic (Stocker et al., 2013; Flato and Marotzke, 2013). Since 1980, the Arctic region has experienced twice the temperature increase compared to the global average (AMAP, 2012). The energy balance in the Arctic can be directly related to changes in sea-ice volume, since it corresponds to changes in latent heat (Schweiger et al., 2011). Latent heat is released when ice forms and taken up when ice melts. The Arctic warming has been most pronounced during autumn, especially in areas where the ice has melted completely during the summer. Open ocean absorbs more heat than ice. The heat is released in the autumn and warms the lower atmosphere (AMAP, 2012). Loss of sea-ice can cause changes in atmospheric circulation and precipitation patterns (Serreze et al., 2007).
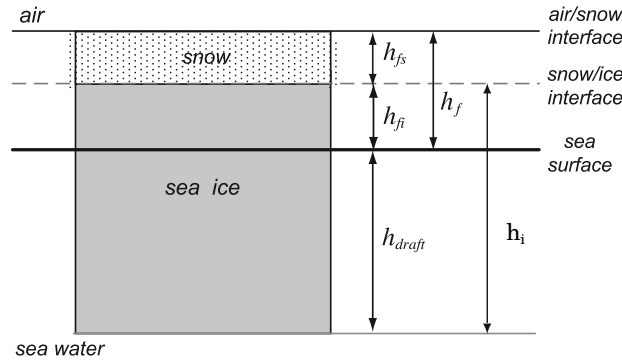

Figure 1: Schematic figure of a sea-ice floe. Note the freeboard h_f, the draft h_{draft} and the ice thickness h_i.
(Kwok and Cunningham, 2008)

IPCC (Vaughan and Comiso, 2013) presents combined data sets of sea-ice draft and thickness from submarine sonars, satellite altimetry, and airborne electromagnetic sensing which compose strong evidence of decreasing Arctic sea-ice thickness over the period 1979-2012. The sea-ice loss has been most evident in September, when the sea-ice typically attains its minimum, although significant decline has been seen all through the year (Stroeve and

Serreze, 2008). Submarine sea-ice draft measurements converted into thickness were the first to show a thickness decrease from the time period 1958-1977 to the mid-1990's. Since 1993, sea-ice freeboard measurements by different satellites(e.g. ESA, ERS, Envisat, ICESat(2003-2009) and CryoSat-2(2012-present)) provide sea-ice thickness data series. Freeboard is the height difference between the snow-air interface and the ocean surface, as seen in Figure 1. Assuming isostatic equilibrium yields the following expression for the sea-ice thickness Equation 1 (Kwok and Cunningham, 2008)

$$h_i = \left(\frac{\rho_w}{\rho_w - \rho_i} \right) h_f - \left(\frac{\rho_w - \rho_s}{\rho_w - \rho_i} \right) h_{fs} \tag{1}$$

where h_i is total sea-ice thickness, h_f is freeboard, h_{fs} is snow thickness, ρ_w is sea water density, ρ_i is ice density and ρ_s is snow density. The freeboard generally accounts for about 10 % of the total thickness (Schweiger et al., 2011). Snow depth is needed to obtain the sea-ice thickness, which can be problematic since continuous snow measurements are not available for the entire Arctic. This can be solved by modelling the snow cover and depth in different ways, as in Kwok et al. (2008) who used daily snow-depth fields from European Centre for Medium-Range Weather Forecasts (ECMWF) snowfall estimates.

Figure 2: Map of the Arctic Basin showing the Transpolar Drift current and the Beaufort Gyre. (NSIDC, 2014)

Repeated electro-magnetic surveys show a thinning of the Transpolar Drift region, see Figure 2. Wind patterns transport sea-ice along this drift, from eastern Siberia towards Fram Strait and out into the Atlantic Ocean (Vaughan and Comiso, 2013). An increase in drift speeds for 2001-2009 has been reported, while the winds during the time period were not particularly strong. This can be explained by thinner sea-ice being more vulnerable to surface wind. One third of the loss of old and thick ice during 2005 and 2008 could be explained by transport of thick multiyear ice from west Canadian Archipelago to the South Beaufort Sea where it melted during summer (Maslanik et al., 2007).

A longer time series for sea-ice volume is now provided by Pan-Arctic Ice-Ocean Modelling and Assimilation System (PIOMAS). Estimates of the sea-ice volume are obtained by a sea-ice-ocean model which describes the sea-ice thickness and extent depending on its response to thermodynamic and dynamic processes (Schweiger et al., 2011). Input of sea surface temperature and sea-ice concentration is provided by atmospheric reanalysis (Notz et al., 2013). The uncertainties in PIOMAS have been evaluated and presented in Schweiger et al. (2011).

1.2.2 Feedbacks and Controls of Sea-Ice Thickness

Serreze et al.(2007) discuss the thermodynamic and dynamic processes underlying the recent decline in sea-ice extent. Thermodynamic processes are related to changes in sea surface temperatures, radiative fluxes and ocean conditions. Dynamic responses in ice circulation are due to changes in ocean and wind currents, e.g. in the location and strength of the Beaufort Gyre, a clockwise motion in western Arctic, and in the Transpolar Drift Stream (Figure 2), which is responsible for most of the ice export though Fram Strait (Serreze et al., 2007).

Observations from satellite and drift buoys do, indeed, show changes in the circulation patterns, with stronger counter-clockwise movements in eastern parts. This makes northward moving multiyear ice to be replaced by first year ice. Multiyear ice is significantly stronger than younger ice, which makes it susceptible for further reductions (Maslanik et al., 2007).

Increased ocean heat transport into the Arctic has been observed. This is an important contribution to the increased melting of the sea-ice. As thin ice insulates less, more ice will be produced during autumn and winter. This causes increased brine release which enhances ocean circulation and a stronger inflow of warm water. Projections show that events of warm water input will get more common in the future (Holland et al., 2006).

Thin ice generally has lower albedo, e.g. reflectivity, than thick ice. This

causes increased radiation absorption which enhances sea-ice melt. This is well-known as the albedo-feedback and has been used as an argument for the possible existence of a so-called tipping point, after which the ice would be unable to recover. Notz (2009) presents stabilizing feedbacks which contradict the existence of a tipping point. Thin ice grows faster than thick ice, which is known as the growth-thickness response. The ocean loses more heat without an insulating ice layer, which in addition to the faster growth also enables ice to form earlier, prolonging growth season. The insulating effect of snow will also decrease since more snow will fall into water than on ice. Increased heat flux from the ocean warms the atmosphere and causes more longwave radiation to be emitted from the top of the atmosphere. As an effect less heat from lower latitudes will be transported into the Arctic by advection.

Modelling experiments by Tietsche et al. (2011) showed that the sea-ice is able to recover to an equilibrium extent within a few years, after the entire sea-ice body was synthetically removed. This equilibrium extent would be determined by the climatic conditions.

The fast growth of thin ice in winter and the increased melt due to lower albedo in the summer causes thin ice to have a greater seasonal cycle. On longer times scales, however, the thicker ice appears to have had the greatest variability. Submarine measurements show a stronger sea-ice reduction where the initial ice was thicker, for the last few decades (Bitz and Roe, 2004). Bitz and Roe found that CMIP models produced the same results for the initial thickness dependent thinning. As the models had weak trends in surface winds or lacked ice dynamics completely, this was explained by thermodynamics.

With an increased radiative forcing the sea-ice tends to adjust its thickness so the annual melt equals the growth. According to Bitz and Roe (2004), the growth is dependent on the thickness, while the melt only shows a minor dependence on the thickness for very thin ice. They show how thick ice is more sensitive to changes in radiative forcing. Bitz (2004) states that ice thinning in the future will be a strong function of the thickness, even without the change in atmospheric circulation which has been seen.

1.2.3 Climate Models

Climate models are used to study the climate and earth-system response to natural and human-induced perturbations. The models are numerical representations of the Earth's natural system (Moss et al., 2010). In atmosphere-ocean circulation models, interactions between atmosphere, ocean, land and sea-ice are simulated. The atmosphere and the ocean are divided into thou-

sands of gridcells for which the different interactions and processes are calculated. These models are highly complex. Regional climate models work in similar ways, but focus on smaller scales and will therefore have a finer resolution.

Earth System Models are based on the physical climate models but do also include ecological and chemical processes, e.g. ocean carbon cycle, vegetation and atmospheric chemistry. Equations are generally simplified and the resolution is coarser than the regional models to enable this many processes to work together. For further details, the reader is referred to Moss et al. (2010). The models are a good way to study the entire earth system and its responses on longer time scales, e.g. century scale or more. Longer time scales are required to capture the long response time of the climate system. Short-term fluctuation can not be tracked, since they are caused by internal, chaotic variability. These short time scales are hence not the focus of classical ESMs (Moss et al., 2010).

The future projections of the models are based on different scenarios describing how e.g. the CO_2 concentration in the atmosphere could change. The research community has identified Representative Concentration Pathways (RCP) describing scenarios and pathways by which certain changes in radiative forcing are reached, according to Table 1 (Moss et al., 2010).

Table 1: The four Representative Concentration Pathways

Name	Radiative forcing	Concentration (p.p.m. CO_2-equiv.)	Pathway
RCP8.5	8.5 Wm^{-2} in 2100	1,370 in 2100	Rising
RCP6.0	6 Wm^{-2} at stabilization without overshoot	850 (at stabilization after 2100)	Stabilization without overshoot
RCP4.5	4.5 Wm^{-2} at stabilization after 2100	650 (at stabilization after 2100)	Stabilization without overshoot
RCP2.6	Peak at 3 Wm^{-2} before 2100 and then declines	Peak at 490 before 2100 and then decline	Peak and Decline

The models evaluated in my thesis are the models from CMIP5. The purpose of these are to provide simulations of climate change and variability for researchers but also to be of interest for national and international assessments of climate scenarios, e.g. IPCC (Taylor, 2012). The experiments in the project have two different time scales. The long-term projections run
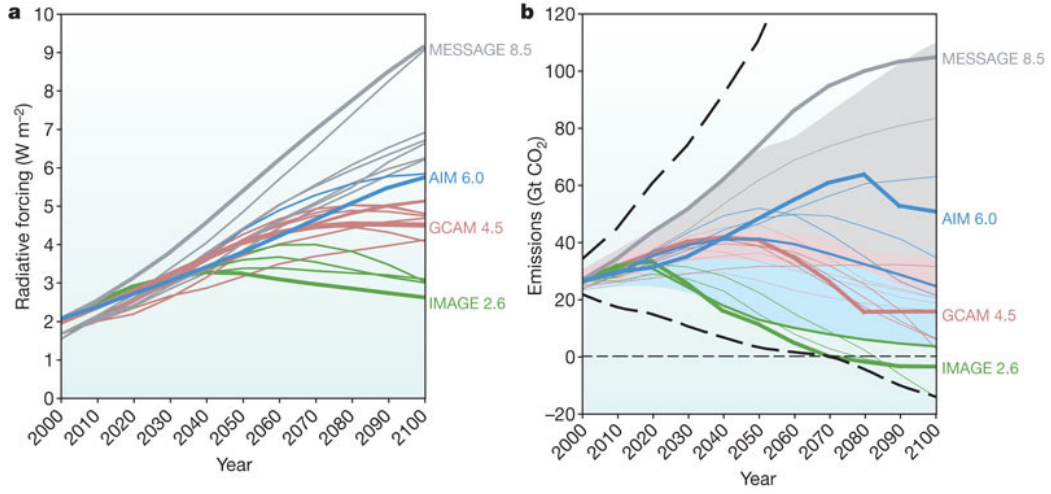
Figure 3: Representative concentration pathways.
a, Changes in radiative forcing relative to pre-industrial conditions. Bold coloured lines show the four RCPs; thin lines show individual scenarios from approximately 30 candidate RCP scenarios.
b, Energy and industry CO_2 emissions for the RCP candidates. The range of emissions is presented for the maximum and minimum (thick dashed curve) and 10th to 90th percentile (shaded area). Blue shaded area corresponds to mitigation scenarios; grey shaded area corresponds to reference scenarios; pink area represents the overlap between reference and mitigation scenarios.
(Moss et al., 2010)

from pre-industrial time, i.e. mid-19th century, through and beyond the 21st century. The near-time projections start mid-20th century and go on until 2035. The models consists of an earth spanning grid. Sea-ice thickness and sea-ice concentration are provided for each grid cell on a monthly and daily basis.

In the EC-EARTH model a dynamic-thermodynamic sea-ice model is used. More information about the model can be found in Koenigk et al. (2013) and articles cited there. The horizontal resolution of the atmospheric component is 1.125° with 62 vertical levels. The ocean component has a horizontal resolution of about 1° with 42 vertical levels. A tri-polar grid is used with the poles over Canada, Siberia and Antarctica (Koenigk et al., 2013).

The sea-ice in MPI-ESM is described in both the ocean and the atmospheric component. The sea-ice component consists of a thermodynamic-dynamic model. The dynamics is based on viscous-plastic rheology. The thermodynamic properties of sea-ice in the model are simplified as described by Notz et al. (2013). The model has two versions with different resolu-

7

tion. The low resolution version MPI-ESM-LR has a horizontal resolution of 1.875° with 47 vertical levels up to 0.7 hPa in the atmospheric part and a horizontal resolution of 1.5° and 40 vertical levels in the ocean part. The poles are positioned over Greenland and Antarctica. The mixed resolution version MPI-ESM-MR has the same horizontal resolution, 1.875°, as LR but with 95 levels in the atmospheric part. In the ocean part the horizontal resolution is changed to 0.4° but the vertical resolution, 40 levels, stays the same as in LR. The MR version has a tripolar grid with the three poles placed in Canada, Siberia and Antarctic (Notz et al., 2013).

The PIOMAS data series for 1979-2013 is used for evaluation of the CMIP5 models. The uncertainties of PIOMAS are discussed by Schweiger et al. (2011), who found that the mean difference between PIOMAS and ICESat was less than 0.1 m. The thickness pattern provided by CryoSat-2 also agrees with PIOMAS's for the winter 2011/2012 and with the growth curve (Laxon et al., 2013). PIOMAS is therefore considered to be adequate for model evaluation in my thesis, although a longer time series would be needed to draw proper conclusion concerning the models' accuracy.

1.3   Aim and Limitations

The aim of this study is to investigate the future evolution of Arctic sea-ice. This is done by comparing the sea-ice output from the CMIP5 models with observations. The focus is on September, when the sea-ice has its minimum. My work will be done around the following questions:

- How does the sea-ice volume produced by the CMIP5 models compare to observations?

- How will the Arctic sea-ice volume change according to the models?
    - What is the evolution of the total sea-ice volume in the Arctic? [Volume Evolution]
    - Do we see a change in the sea-ice volume seasonal cycle? [Seasonal Cycle]
    - Where is the change in sea-ice thickness most pronounced? [Spatial variability]

2   Method

The monthly sea-ice data from the CMIP5 models was analysed and compared to PIOMAS. Three RCP scenarios were used: the mitigation scenario RCP2.6, the medium stabilization scenario RCP4.5 and the high emission scenario RCP8.5. Data from the intermediate scenario (RCP6.0) was not available and therefore not included in the study.

The CMIP5 models provide monthly sea-ice thickness (SIT) and sea-ice concentration (SIC). SIT is the average thickness over the grid cell, as described by Notz (2013). The analysis was performed with Climate Data Operators (CDO), maps produced with the NCAR Command Language (NCL) and figures were made in MATLAB. Since this thesis focuses on the Arctic sea-ice, a region from 65°N and northward was chosen in the analysis.

Sea-ice volume (SIV) and sea-ice real thickness (SIRT) was calculated according to.

$$SIV = SIT \cdot gridarea \tag{2}$$

$$SIRT = SIT \cdot SIC \tag{3}$$

SIRT is the mean thickness of the ice, whereas SIT is the average which is taking SIC into account. Changes in SIT can therefore be interpreted as changes in volume while SIRT provides a more correct value of the actual thickness.
To exclude unrealistic values produced by the models CCSM4, HadGEM2-CC, GFDL, MRI-CGCM3 and NorESM1, a valid range of 0 to 10 m for the sea-ice thickness was set.

2.1   Included Models and Runs

Since the focus in this thesis is on the time periods 1850-2005 and 2006-2100, only the models and runs covering these periods were analysed for their volume evolution and seasonal cycle. These were the following 14 long-term models: ACCESS1, bcc-csm1-1, CanESM2, CCSM4, CNRM-CM5, CSIRO-Mk3-6-0, EC-EARTH, IPSL-CM5A-LR, IPSL-CM5A-MR, IPSL-CM5B-LR, MPI-ESM-LR, MPI-ESM-MR, MRI-CGCM3 and NorESM1-ME.

A total of 22 models, including short-term models, were represented in the scatter plot displaying the mean volume and volume trend over the time periods 1976-2005 and 2006-2035 (section 3.1). The 8 additionally included short-term models were: CanCM4, HadCM3, HadGEM2-CC, HadGEM2-ES, MIROC4h, MIROC5, MIROC-ESM-CHEM and MIROC-ESM.

The model inmcm4 was not included in any analysis since it produced volumes and trends which were two orders of magnitude out of range. Some EC-EARTH runs, see Table 2, were excluded from all analysis. These runs had the same seasonal cycle year after year. Despite this, they are shown in the scatter plot where their trend is zero.

Table 2: Excluded EC-EARTH runs

Historical	RCP2.6	RCP4.5	RCP8.5
r7, r11, r13	r3, r11	r12	r3, r7, r9, r10, r11, r12, r13

2.2 Volume Evolution

The September sea-ice evolution was evaluated for the time period 1850-2100. The period 1850-2005 is referred to as the historical period. The following period, 2006-2100, is covered by the three scenarios RCP2.6, RCP4.5 and RCP8.5. The multi-model mean, MPI-ESM mean and EC-EARTH mean together with 10 year running means were calculated. The PIOMAS data series has daily output instead of monthly. For proper comparisons the September mean volume was calculated.

To evaluate the spread of the models, their mean volume and mean volume trend over 1976-2005 (historical) and 2006-2035 (RCP2.6, RCP4.5 and RCP8.5) were compared in a scatter plot (section 3.1). The mean and trend of the long-term models used in the rest of the thesis were calculated. The models covering shorter time periods were represented in this plot, but not used in the calculations.

2.3 Seasonal Cycle

The change in the seasonal cycle was examined by comparing the monthly means over 15 year periods. Pre-industrial time (1851-1865), the end of the historical time period (1991-2005) and the end of the future projection (2086-2100) from the three RCP scenarios were analysed. The seasonal cycle from PIOMAS (1979-2013) was used as comparison.

The annual volume change was calculated as the difference between the annual maximum and minimum. The models used in the previous section were used here. The volume change for PIOMAS was calculated as the difference between the mean March volume and the mean September volume.

2.4 Spatial Variability

To answer the question of where most ice loss will occur, maps of the sea-ice thickness were produced in NCL. Since the area of the grid cells decreases towards the poles the thickness was displayed instead of the volume, as the volume is dependent on the area. It is also easier to interpret changes in thickness rather than volume.

The models have different grids which makes it hard to merge them into an ensemble, therefore only EC-EARTH and the mixed resolution version MPI-ESM-MR were evaluated in this part. The sea-ice thickness evolution in September was represented by the mean thickness over a few time periods. 1851-1865, 1956-1975, 1991-2005 from the historical time period. The RCP4.5 simulations were used to represent the future projections for the time periods 2006-2020, 2051-2065 and 2086-2100. Maps describing the thickness change through the historical time period and the RCP4.5 time period were made.

The change in the real thickness over the historical time period was then compared in a scatter plot against the initial real thickness for the two models.

3 Results

3.1 Volume Evolution

The evolution of the total sea-ice volume in the Arctic region is seen in Figure 4. The top figure shows the model mean. A few models had runs which did not cover both the historical and the RCP time period. Therefore a small offset is seen around year 2005-2006.

The ensemble of models shows a small decrease starting already before 1900, but it is enhanced during the last part of the historical run. The magnitude of the volume compares well with PIOMAS until the start of the RCP scenarios, where PIOMAS shows a rapid decrease which is not seen in the models.
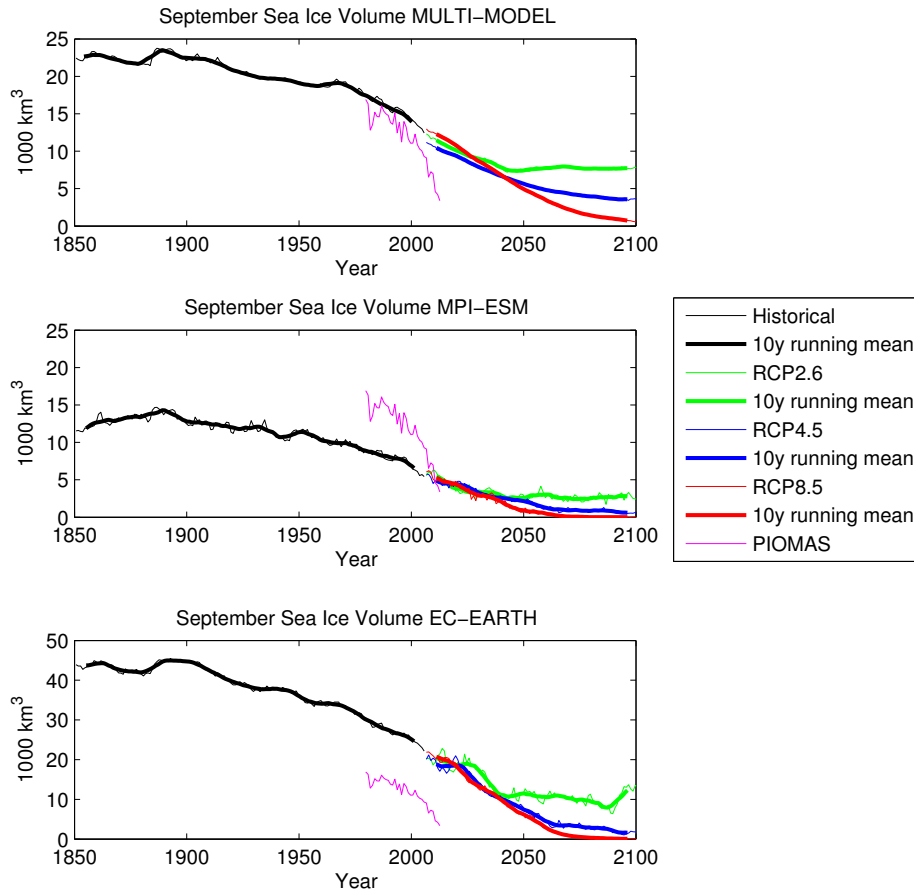

Figure 4: Total sea-ice volume in the Arctic region, according to the MULTI-MODEL mean, MPI-ESM and EC-EARTH.
Note that the scale for EC-EARTH is different!

12

The MPI-ESM model shows a decline in sea-ice volume starting already before the year 1900 and continuing through the historical period and the first part of the RCP period. The RCP scenarios split up first after 2030, when RCP2.6 stabilizes around $2.5 \cdot 10^3$ km^3. RCP4.5 does not stabilize but the decrease slows down after 2050 while RCP8.5 continues the rapid decrease towards an ice free September around 2070. MPI-ESM underestimates the volume compared to PIOMAS until the last few years. The drastic decrease seen in PIOMAS is not seen in any of the RCP projections.

EC-EARTH shows a continuous decrease in sea-ice volume from around the year 1900 onwards. The RCP scenarios follow the same trend as the historical simulations until RCP2.6 stabilizes, around year 2040. RCP8.5 continues the decreasing trend until it reaches ice-free conditions. RCP4.5 also continues to decrease, but the trend is less steep after 2060.

The mean volume and the volume trend for all the models during the time periods 1976-2005 and 2006-2035 are presented in Figure 5. With the historical time period in (a) PIOMAS is also presented although it starts in 1979. PIOMAS lies within the CMIP5 standard deviation of the volume, but none of the CMIP5 models is able to reproduce its trend.

The MPI-ESM runs underestimates the volume compared to the long-term models' mean and PIOMAS, although they mostly lie within the standard deviation. The trends are spread out within the standard deviation of the long-term models. The EC-EARTH runs overestimate the mean volume compared to the model mean and PIOMAS. The trends show large variability, from close to zero to among most rapid decreasing.

MPI-ESM and EC-EARTH compare in the same manner to the other models in the RCP simulations, seen in Figure 5 (b), (c) and (d). The multi-model mean trend is stronger for higher RCP, but the mean volume is highest for the RCP8.5.

EC-EARTH runs with a trend of zero are seen for all scenarios in Figure 5. These models were excluded as mentioned in Section 2.2.

3.2   Seasonal Cycle

The change of the seasonal cycle in the model ensemble, EC-EARTH and MPI-ESM is presented in Figure 6. The multi-model mean matches the magnitude of the winter volume well, but overestimates the volume during the summer. The start of the melting season is later than seen in PIOMAS.

EC-EARTH overestimates the volume, especially during summer. It displays a shift in the seasonal cycle towards an earlier melt-season start. The maximum for the pre-historical time period occurs in June while it for the

13
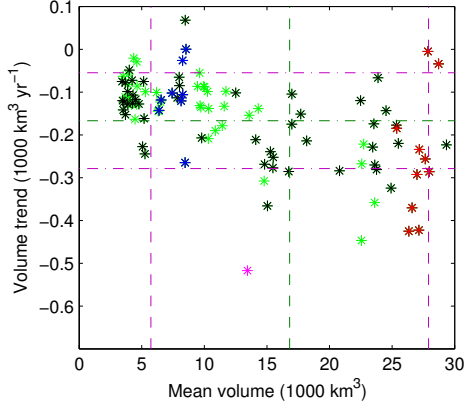
(a) Historical 1976-2005
The mean volume for all the models is
$16.8 \cdot 10^3 \text{km}^3$ with the standard deviation
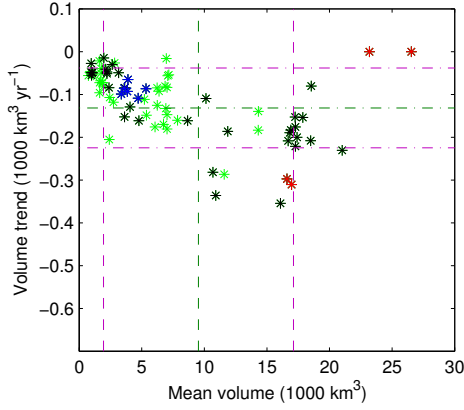$11.1 \cdot 10^3 \text{km}^3$.
The mean trend is $-0.17 \cdot 10^3 \text{km}^3 \text{yr}^{-1}$ with
the standard deviation $0.12 \cdot 10^3 \text{km}^3 \text{yr}^{-1}$.
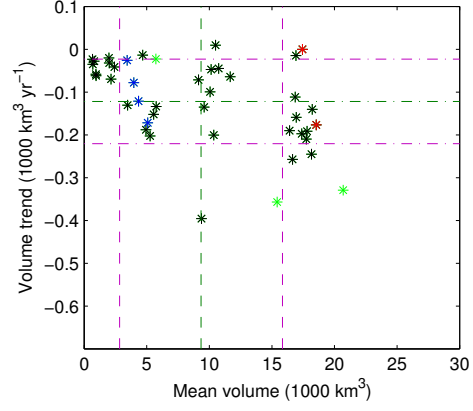
(b) RCP2.6 2006-2035
The mean volume for all the models is
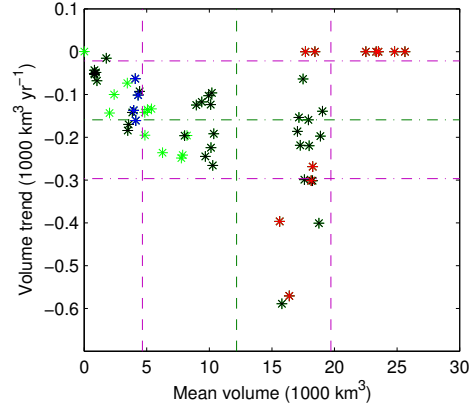$9.5 \cdot 10^3 \text{km}^3$ with the standard deviation
$6.5 \cdot 10^3 \text{km}^3$.
The mean trend is $-0.12 \cdot 10^3 \text{km}^3 \text{yr}^{-1}$ with
the standard deviation $0.09 \cdot 10^3 \text{km}^3 \text{yr}^{-1}$.

(c) RCP4.5 2006-2035
The mean volume for all the models is
$9.5 \cdot 10^3 \text{km}^3$ with the standard deviation
$7.6 \cdot 10^3 \text{km}^3$.
The mean trend is $-0.13 \cdot 10^3 \text{km}^3 \text{yr}^{-1}$ with
the standard deviation $0.093 \cdot 10^3 \text{km}^3 \text{yr}^{-1}$.

(d) RCP8.5 2006-2035
The mean volume for all the models is
$12.2 \cdot 10^3 \text{km}^3$ with the standard deviation
$7.5 \cdot 10^3 \text{km}^3$.
The mean trend is $-0.16 \cdot 10^3 \text{km}^3 \text{yr}^{-1}$ with
the standard deviation $0.14 \cdot 10^3 \text{km}^3 \text{yr}^{-1}$.

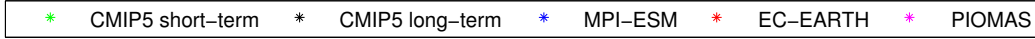| * | CMIP5 short–term | * | CMIP5 long–term | * | MPI–ESM | * | EC–EARTH | * | PIOMAS |

Figure 5: The September sea-ice volume mean (x-axis) and trend (y-axis) for the CMIP5
models, and their runs, for the time periods 1976-2005 and 2006-2035. The dashed lines
symbolizethe mean and standard deviation of all the long term models' volumes and
volume trends.

14

late RCP's occurs in April or May. The season cycle from MPI-ESM has a good timing compared with PIOMAS, but underestimates the volume.
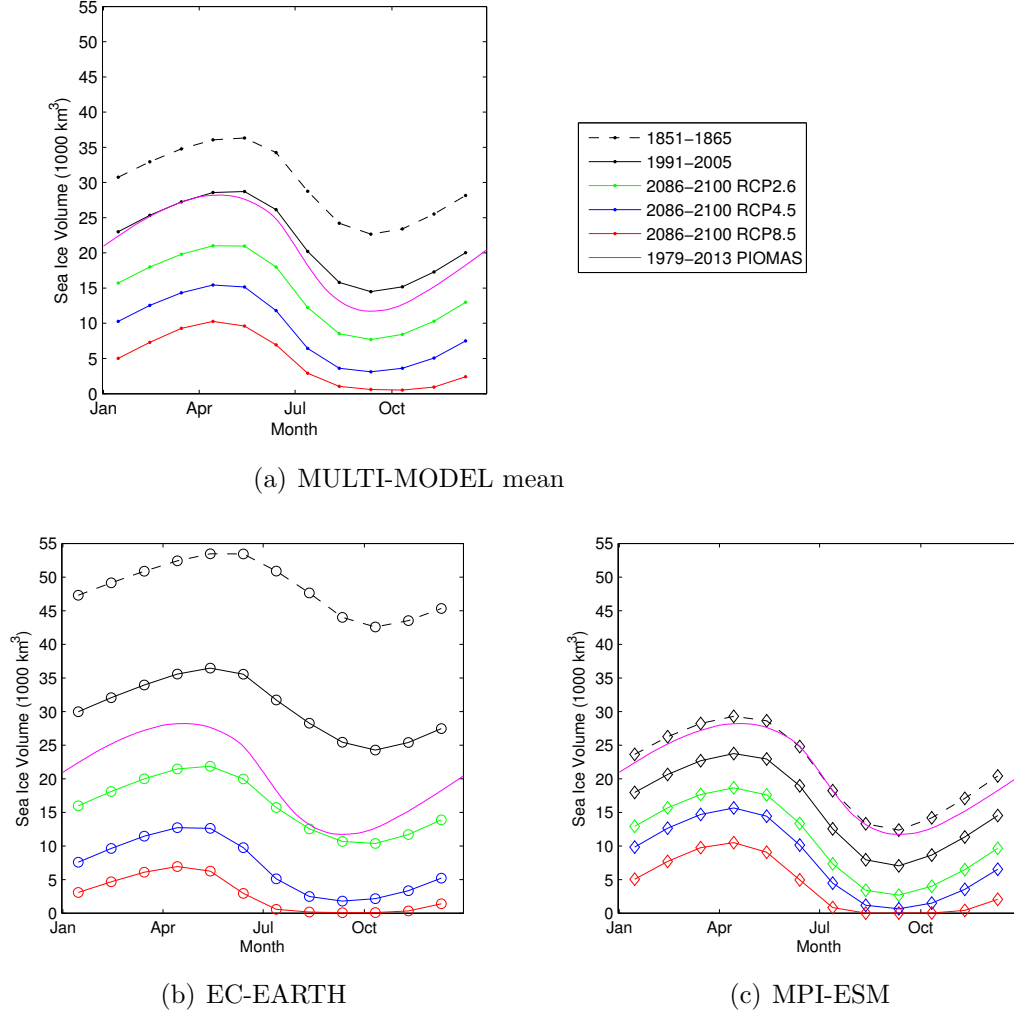

(a) MULTI-MODEL mean

(b) EC-EARTH

(c) MPI-ESM

Figure 6: The mean seasonal cycle of sea-ice volume (1000 km^3) provided by the multi-model mean, EC-EARTH and MPI-ESM for the time periods 1851-1865, 1991-2005 and 2086-2100. The mean seasonal cycle from PIOMAS for the time period 1979-2013 is also represented.

The annual sea-ice volume change is the amount of ice which is melting each year. The change over time according to the multi-model mean, MPI-ESM, EC-EARTH and PIOMAS is presented in Figure 7. The annual volume change stays relatively constant for the multi-model mean and MPI-ESM, while EC-EARTH shows a slight increase. All three have a pronounced decrease in volume change for the last part of the RCP8.5 projection. The
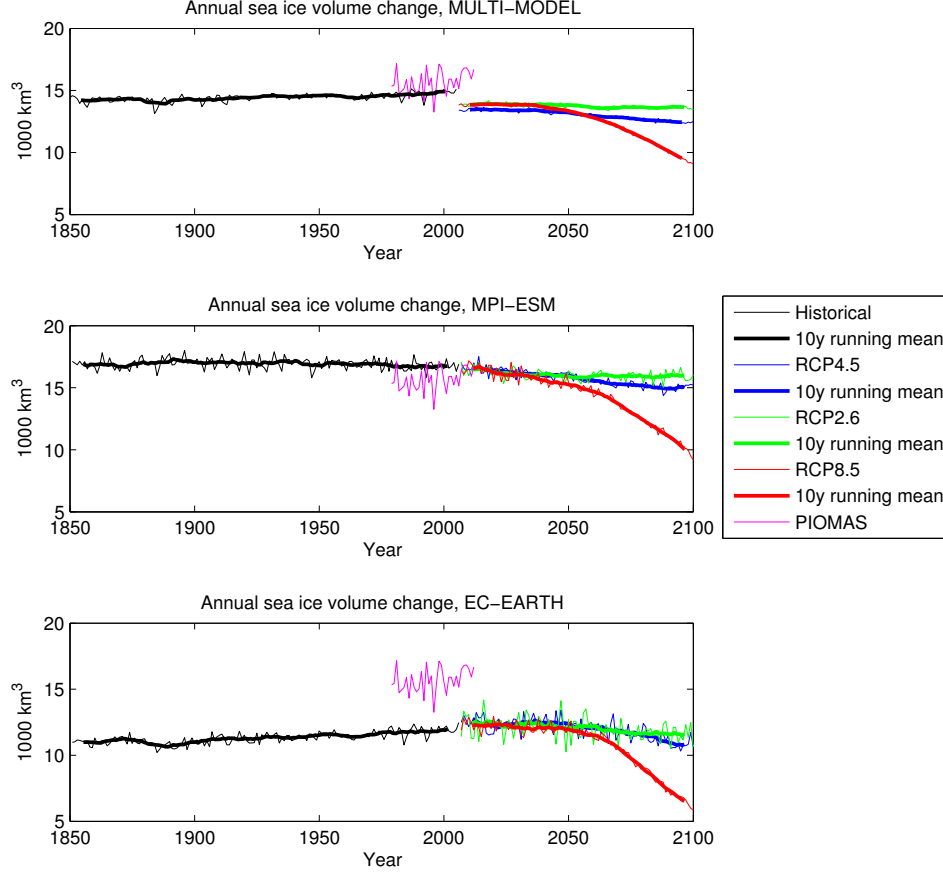
15

Figure 7: Annual change in sea-ice volume presented for the multi-model mean, MPI-ESM and EC-EARTH. The change represents the annual loss, which was calculated by subtracting the annual minimum value from the annual maximum value.

magnitude of the multi-model mean and MPI-ESM compare well with PI-OMAS, while EC-EARTH underestimates it.

3.3   Spatial Variability

The September sea-ice thickness evolution from EC-EARTH is presented in Figure 8. A continuous decrease in thickness can be seen throughout the time period. The thickest ice at the start of the historical time period is found north of Greenland, northern Arctic Canada and north of western Siberia.

The thickness change between the start and end of the historical time period by EC-EARTH is presented in Figure 9(a) and for the RCP4.5 run in Figure 9(b). The greatest thickness loss takes place north and north-west
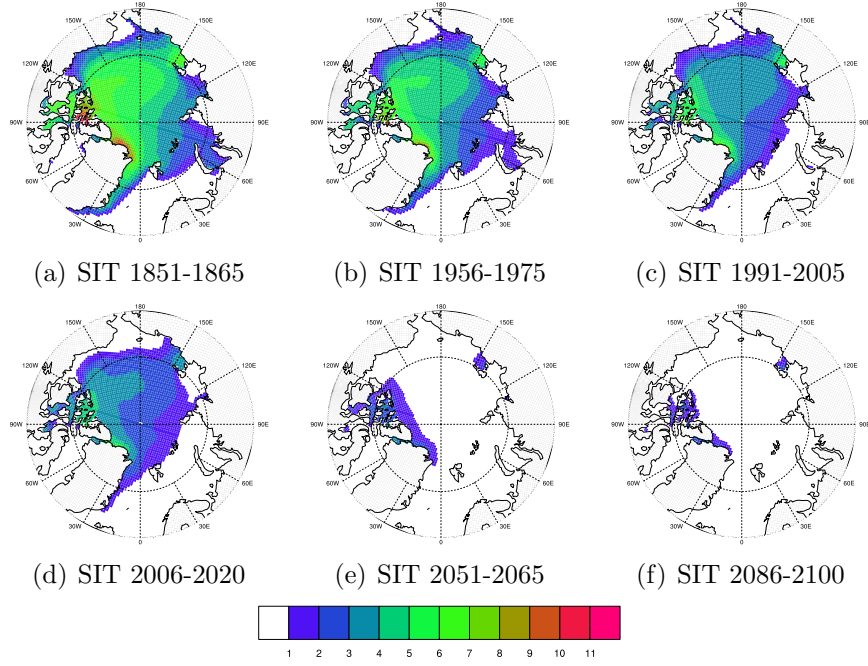
16

(a) SIT 1851-1865   (b) SIT 1956-1975   (c) SIT 1991-2005

(d) SIT 2006-2020   (e) SIT 2051-2065   (f) SIT 2086-2100

Figure 8: Sea-ice thickness (m) from EC-EARTH. The scale is from 0 to 11 m.

(a) SIT change from 1850-1865 to 1991-2005

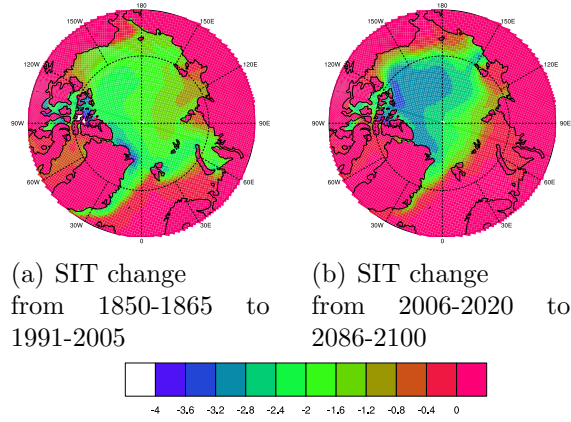(b) SIT change from 2006-2020 to 2086-2100

Figure 9: Sea-ice thickness change (m) by EC-EARTH. The scale is from -4 to 0 m.

of Greenland, in north-western Canadian Arctic and north-west of Svalbard for the historical time period. The pattern for the RCP4.5 time period is similar, but with more thinning in the central Arctic.

Figure 10 shows the September sea-ice thickness evolution according to MPI-ESM. The thickest ice is found north of Greenland and western hemisphere central Arctic. A distinct thickness decrease is seen together with a drastic decrease in sea-ice extent, especially during the RCP4.5 simulation.
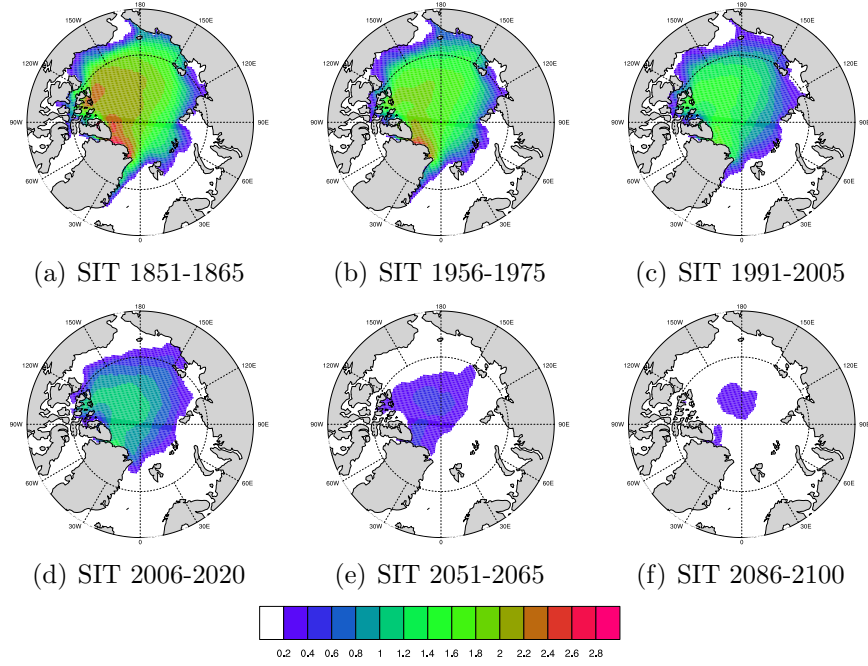
17

(a) SIT 1851-1865   (b) SIT 1956-1975   (c) SIT 1991-2005

(d) SIT 2006-2020   (e) SIT 2051-2065   (f) SIT 2086-2100

0.2 0.4 0.6 0.8 1 1.2 1.4 1.6 1.8 2 2.2 2.4 2.6 2.8

Figure 10: Sea-ice thickness by MPI-ESM-MR. The scale is from 0 to 2.8 m.

(a) SIT change from 1850-1865 to 1991-2005

(b) SIT change from 2006-2020 to 2086-2100

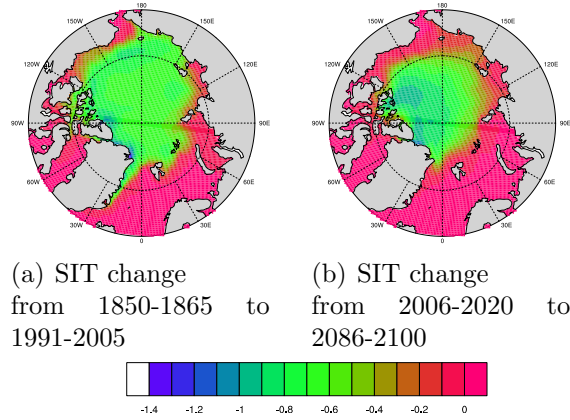-1.4   -1.2   -1   -0.8   -0.6   -0.4   -0.2   0

Figure 11: Sea-ice thickness change by MPI-ESM-MR. The scale is from -1.4 to 0 m.

In Figure 11 the thinning during the historical time period (a) and the RCP4.5 period (b), is presented. The pattern of thinning is very similar to what is seen for EC-EARTH, although the sea-ice is significantly thicker in EC-EARTH.

The sea-ice thickness from PIOMAS for the period 1979-2007 is presented in Figure 12. The thickness lies between EC-EARTH and MPI-ESM, but the distribution of thick ice is better represented by EC-EARTH (except for west
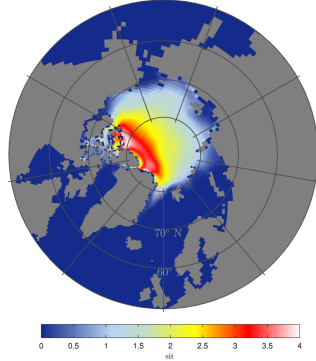
Figure 12: Map of the September sea-ice thickness (m) from PIOMAS over the period 1979-2007. The scale is from 0 to 4 m. (Notz et al., 2013)

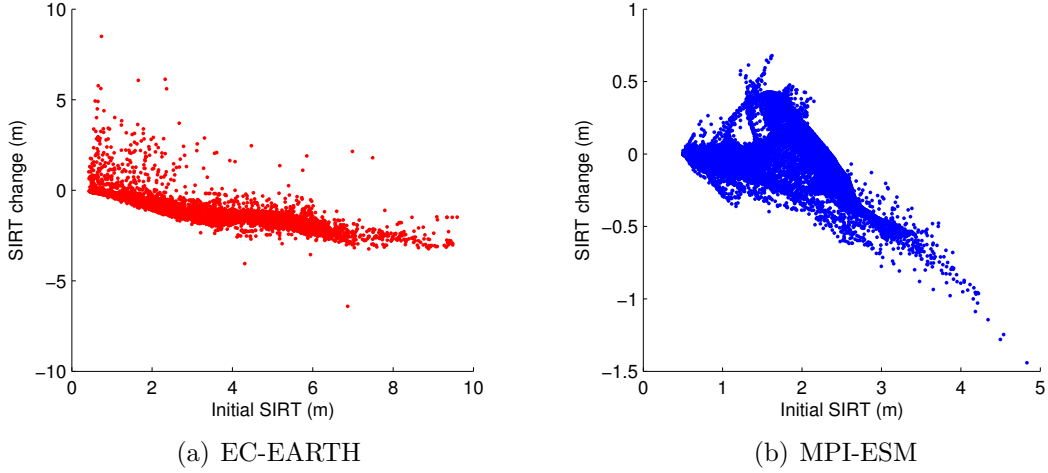of Novaya Zemlya, Arctic Siberia, where thick ice appear to be trapped).

(a) EC-EARTH

(b) MPI-ESM

Figure 13: The initial real thickness, on the x-axis, is the mean sea-ice September thickness during the time period 1851-1865. The thickness change from this time period until 1991-2005 is represented on the y-axis. Each dot represents one gridcell.

In Figure 13 the September mean sea-ice real thickness for the start of the historical time period, 1851-1865, is plotted against the real thickness change from this time period to the end of the historical time period, 1991-2005. SIRT is used in this part to display the thickness without influences from the changes in the sea-ice concentration. The two models both have most thinning where the ice initially was thickest.

EC-EARTH and MPI-ESM provide two different scenarios of where the last ice will be found at the end of the RCP4.5 run. EC-EARTH predicts it where the ice was initially thickest while MPI-ESM predict it to be in the very central Arctic.

4 Discussion

First I will discuss the models, how they compare to PIOMAS and in what circumstances they could be trusted. Thereafter I will discuss what predictions can be made according to this.

4.1 Evaluation of Models

The multi-model mean compares relatively well with PIOMAS until the RCP-period starts, where the models cannot reproduce the rapid decline. MPI-ESM underestimates the volume while EC-EARTH overestimates it. EC-EARTH appears to reproduce the decreasing trend best. The annual cycle for PIOMAS has increased during recent time with the rapid volume decline. This implies increased melt and growth, which could be expected of a thinner ice cover as described by Bitz and Roe (2004). Such change in the annual cycle is not seen for the model ensemble, MPI-ESM or EC-EARTH.

Neither the multi-model mean, MPI-ESM or EC-EARTH matches both magnitude and timing of the seasonal cycle compared to PIOMAS. The volume is best represented by the multi-model mean but MPI-ESM provides better timing.

During the time of the ICESat operations the spring multiyear sea-ice thinned by 0.6 m, while the first year ice showed a negligible trend. The autumn(Oct/Nov) volume between 2003-2008 decreased by 1237 km^3y^{-1} (Vaughan and Comiso, 2013). This is an even stronger decrease than seen in PIOMAS.

The models can reproduce different sea-ice features and processes, e.g. the timing and magnitude of the seasonal cycle, but not when it comes to producing the rapid decline for the last years. The sea-ice components of the models are simplified and this could cause some errors. Extreme internal variability in the earth system right now could explain some of the decline and would not be reproduced by the models. Thought, the magnitude of the decline indicates that there is something missing in the models. This is taken into account when discussing the future in next section.

4.2 Future Predictions

The future of the sea-ice depends on how the radiative forcing, thus the emissions of greenhouse gases, will change. The models indicate that the sea-ice volume has some kind of quasi-equilibrium which is dependent on the climatic conditions. Out of the three RCP scenarios in this thesis only

20

the high-emission scenario RCP8.5 reaches ice-free conditions in September before 2100. Though, individual models get ice-free conditions even in the RCP4.5 scenario.

Massonnet et al. (2012) investigated when ice-free summer conditions would be reached according to the CMIP5 models. This results showed that ice-free summer would occur between 2040 and sometime after 2100 with the RCP4.5 projection and between 2041 and 2060 with the RCP8.5 projection. The sea-ice so far has reacted stronger than simulated by the models. Since the volume is lower and the reduction faster than seen in the models, ice-free conditions could be expected earlier than predicted.

The models show the sea-ice would be able to stabilize around a quasi-equilibrium depending on the climatic forcings. Tietsche et al. (2011) showed in their modelling experiments that even if the sea-ice disappeared it would come back if the climate got cooler. The models do not indicate a tipping point below which the ice loss would be unstoppable and irreversible, which supports that the sea-ice would be able to come back.

MPI-ESM-MR and EC-EARTH both indicate that the ice is thinning more where it initially was thickest, which is in line with what observations show (Bitz and Roe, 2004). The two models do not agree on how the ice would thin during the second half of the RCP4.5 scenario. MPI-ESM-MR suggests that the last ice would occur in the central Arctic region. This is not very likely without a change in the pattern in ocean circulation and currents. As seen in Figure 2 the Transpolar Drift is strong in this region. Thin ice is more vulnerable to external forcings, such as winds and currents. Differences between the two models in these components could explain the difference seen.

It is possible that the rapid decrease that has been seen over the last years will diminish when most of the thicker ice has melted away. Thicker ice should be more sensitive to changes in radiative forcing according to theory(Bitz and Roe, 2004), observations and the models evaluated in this thesis.

5 Conclusion

There are many indications that the current sea-ice volume can not simply be linearly extrapolated down towards ice-free conditions. The reduction will probably slow down when the ice gets thinner and most multi-year ice is lost. According to the evaluated models, the sea-ice will find a new quasi-equilibrium depending on climatic conditions. This implies that - if we are able to reduce, stop or reverse our greenhouse gas emissions and the global warming - the sea-ice will be able to recover.

The models inability to reproduce the current decline indicate that there is some component missing in the models. The evolution towards ice-free summer conditions will probably be faster than seen in the models.

6 Outlook

There are many possibilities for further investigations following this thesis. The main finding in this thesis is that there is some component missing in the models. This implies that further development of the models is required. There may be a fundamental aspect in sea-ice physics which is not known to us, thus it is of great importance to continue research about the basics of sea-ice physics.

Continued investigation in the line of this thesis could include following aspects:

- The focus in this thesis was on September, but it would be interesting to do the same evaluation in March/April, when the sea-ice has its maximum.

- The growth/melt season length could not be evaluated since the change would not be seen for monthly data. There is an opportunity to look further into that using daily data.

- By formulating a relationship between volume change and thickness, further predictions of the sea-ice evolution could be made. This would probably be more representative than any linear or exponential fits.

- Maps showing the multi-model mean thickness, as made here fore MPI-ESM-MR and EC-EARTH, would be more representative. This requires re-gridding of the models into a common grid.

7   Self-Reflection

By doing this thesis I have increased my understanding and knowledge about the relationship between the climate system and the Arctic sea-ice. The ability to use climate data operators and write scripts makes analysis of climatic data sets possible.

The full process of choosing topic, planning the work, doing the analysis and writing the report has been an important learning outcome.

8   Abbreviations

CMIP5	Coupled Modelling Comparison Project 5
EC-EARTH	European Centre for Medium-range Weather Forecast's earth system model
IPCC	The Intergovernmental Panel on Climate Change
MPI-ESM	Max Planck Institute for Meteorology's Earth System Model
PIOMAS	Pan-Arctic Ice-Ocean Modelling and Assimilation System, reanalysis data series of sea-ice thickness
RCP	Representative Concentration Pathway
SIC	Sea-Ice Concentration
SIRT	Sea-Ice Real Thickness, the mean thickness of the ice
SIT	Sea-Ice Thickness, the average thickness of ice, accounting for the sea-ice concentration
SIV	Sea-Ice Volume

9 Bibliography

AMAP (2012) Arctic Climate Issues 2011: Changes in Arctic Snow, Water, Ice and Permafrost. SWIPA 2011 Overview Report.

Bitz, CM and Roe, GH (2004) A Mechanism for the High Rate of Sea Ice Thinning in the Arctic Ocean, *American Meteorological Society*, 17, 3623-3632.

Holland, MM, Bitz, CM and Tremblay, B (2006) Future abrupt reductions in the summer Arctic sea ice, *Geophys Res Lett*, 33(23), L23503.

Flato, G and Marotzke, J (2013) Chapter 9: Evaluation of Climate Models In: *Climate Change 2013: The Physical Science Basis. Contribution of Working Group I to the Fifth Assessment Report of the Intergovernmental Panel on Climate Change*, Cambridge University Press, Cambridge, United Kingdom and New York, NY, USA.

Koenigk, T, Brodeau, L, Grand, R, Wyser, K and Wille, U (2013) Arctic climate change in 21st century CMIP5 simulations with EC-Earth, *Clim Dyn*, 40, 2719-2743.

Kwok, R and Cunningham, GF (2008) ICESat over Arctic sea ice: Estimation of snow depth and ice thickness, *J Geophys Res*, 113, C08010.

Laxon, SW, Giles, KA, Ridout, Andy L, Wingham, DJ, Willatt, R, Cullen, R, Kwok, R, Schweiger, A, Zhang, J, Haas, C, Hendricks, S, Krishfield, R, Kurtz, N, Farrell, S and Davidson, M (2013) CryoSat-2 estimates of Arctic sea ice thickness and volume, *Geophys Res Lett*, 40, 732-737.

Maslanik, JA, Fowler, C, Stroeve, J, Drobot, S, Zwally, J, Yi, D and Emery, W (2007) A younger, thinner Arctic ice cover: Increased potential for rapid, extensive sea-ice loss, *Geophys Res Lett*, 34(24), L24501.

Massonnet, F, Fichefet, T, Goosse, H, Bitz, CM, Philippon-Bertier, G, Holland, MM and Barriat, P-Y (2012) The Cryosphere Constraining projections of summer Arctic sea ice, *The Cryosphere*, 6, 1383-1394.

Moss, RH, Edmonds, JA, Hibbard, KA, Manning, MR, Rose, SK, van Vuuren, DP, Carter, TR, Emori, S, Kainuma, M, Kram, T, Meehl, GA, Mitchell, JFB, Nakicenovic, N, Riahi, K, Smith, SJ, Stouffer, RJ, Thomson, AM, Weyant, JP and Wilbanks, TJ (2010) The next generation of scenarios for climate change research and assessment, *Nature*, 463(7282), 747-56.

Notz, D (2013) Sea-ice extent provides a limited metric of model performance, *The Cryosphere Discussions*, 7, 3095-3131.

Notz, D (2009) The future of ice sheets and sea ice : Between reversible retreat and unstoppable loss, *PNAS*, 106(49), 20590-20595.

Notz, D, Haumann, FA, Haak, H and Jungclaus, JH (2013) Arctic sea-ice evolution as modeled by Max Planck Institute for Meteorology's Earth system model 1, *Journal of*

Advances in Modeling Earth Systems, 5, 173-194.

Schweiger, A, Lindsay, R, Zhang, J, Steele, M, Stern, H and Kwok, R (2011) Uncertainty in modeled Arctic sea ice volume, *J Geophys Res*, 116, C00D06.

Serreze, MC, Holland, MM and Stroeve, J (2007) Perspectives on the Arctic's shrinking sea-ice cover, *Science*, 315(5818), 1533-6.

Stocker, TF, Qin, D, Plattnet, G-K, Tignor, M, Allen, SK, Boschung, J, Nauls, A, Xia, Y, Bex, V and Midgley, PM (eds.) (2013) Summary for Policymakers. In: *Climate Change 2013: The Physical Science Basis. Contribution of Working Group I to the Fifth Assessment Report of the Intergovernmental Panel on Climate Change*, Cambridge University Press, Cambridge, United Kingdom and New York, NY, USA.

Stroeve, JC, Serreze, MC, Holland, MM, Kay, JE, Malanik, J and Barrett, AP (2011) The Arctic's rapidly shrinking sea ice cover: a research synthesis, *Clim Change*, 110(3-4), 1005-1027.

Stroeve, J and Serreze, MC (2008) Arctic Sea Ice Extent Plummets in 2007, *EOS, Transactions, American Geophysical Union*, 89(2), 13-14.

Taylor, KE, Stouffer, RJ and Meehl, GA (2012) An Overview of CMIP5 and the Experiment Design, *Bulletin of the American Meteorological Society*, 93(4), 485-498.

Tietsche, S, Notz, D, Jungclaus, JH and Marotzke, J (2011) Recovery mechanisms of Arctic summer sea ice, *Geophys Res Lett*, 38, L02707.

Tietsche, S, Notz, D, Jungclaus, JH and Marotzke, J (2013) Predictability of large interannual Arctic sea-ice anomalies, *Clim Dyn*, 41(9-10), 2511-2526.

Vaughan, DG and Comiso, JC (2013) Chapter 4: Observations: Cryosphere In: *Climate Change 2013: The Physical Science Basis. Contribution of Working Group I to the Fifth Assessment Report of the Intergovernmental Panel on Climate Change*, Cambridge University Press, Cambridge, United Kingdom and New York, NY, USA.

National Snow and Ice Data Centre (NSIDC): All About Sea Ice, Accessed 7 January 2014, <http://nsidc.org/cryosphere/seaice/processes/circulation.html>